Kapaca, E.; Jiang, J.; Cho, J.; Jorda Moret, JL.; Díaz Cabañas, MJ.; Zou, X.; Corma Canós, A.... (2021). Synthesis and Structure of a 22 x 12 x 12 Extra-Large Pore Zeolite ITQ-56 Determined by 3D Electron Diffraction. Journal of the American Chemical Society. 143(23):8713-8719. https://doi.org/10.1021/jacs.1c02654

Synthesis and structure of a 22×12×12 extra-large pore zeolite ITQ-56 determined from continuous rotation electron diffraction data

Elina Kapaca[†,#], Jiuxing Jiang[§,#], Jung Cho[†], Jose L. Jorda[⊥], Maria J. Diaz-Cabañas[⊥], Xiaodong Zou[†], Avelino Corma[⊥,*], Tom Willhammar[†,*]

[†]Department of Materials and Environmental Chemistry, Stockholm University, SE-106 91 Stockholm, Sweden

[§]MOE Key Laboratory of Bioinorganic and Synthetic Chemistry, School of Chemistry, Sun Yat-Sen University, Guangzhou 510275, China

[⊥]Instituto de Tecnología Química, Universitat Politècnica de València-Consejo Superior de Investigaciones Científicas, Avenida de los Naranjos s/n, 46022 Valencia, Spain

# These authors contributed to the work equally.

ABSTRACT

A multi-dimensional extra-large pore zeolite, denoted ITQ-56, has been synthesized by using modified memantine as an OSDA (organic structure directing agent). ITQ-56 crystallizes as plate-like nanocrystals. Its structure was determined by continuous rotation electron diffraction (cRED). The structure of ITQ-56 contains extra-large 22-ring and straight intersecting 12-ring channels. The framework density is as low as 12.4 T atoms/1000Å^3. The discovery of ITQ-56 structure not only fills the missing member of extra-large pore zeolite with 22-ring channels, but also opens a new way of making extra-large pore zeolites.

INTRODUCTION

Zeolites are crystalline microporous materials that consist of corner-sharing tetrahedral (TO_4) units (T = Si, Al, Ge, Ga, P, Be, Ga, B etc.) and well-defined pore structures at molecular scale. Zeolites are classified by the number of T-atoms delimiting the pore openings as small (8-ring), middle (10-ring), large (12-ring) and extra-large (>12-ring) pore zeolites. They are used in a wide range of applications in catalysis, gas separation, ion exchange etc. Great efforts have been made to target synthesis processes that can lead to zeolites with extra-large pores, specific composition[1] and functional oriented cavities.[2] Ten years ago, we published a review article[3] to summarize the synthesis, structure, and catalytic behavior of extra-large pore zeolites. One of the strategies was to combine the use of an inorganic structure directing agent, germanium, and large/rigid organic structure directing agents (OSDAs). This has resulted, up to now, in more than 10 new zeolite structures. The introduction of germanium prompted the formation of *d*4*rs* (double 4-rings) and therefore extra-large pores in the structures. Interestingly, the presence of *d*4*rs* in germanosilicate zeolites has opened another approach of making new zeolites, i.e. via the Assembly-Disassembly-Organization-Reassembly (ADOR) approach.[4] Wu et al.[5] successfully prepared a 14×10-ring extra-large pore zeolite ECNU-9 by interlayer expansion. Recently, Camblor et al.(*Angew. Chem. Int. Ed.* **2021**, *60*, 3438-3442) presented an interesting zeolite HPM-14 with interconneceted extra-large and odd small ring (16×9×8) channel system. Despite the large efforts, zeolites with extra-large pores are still rare. The pore opening of all reported extra-large pore zeolites ranges from 14- to 30-ring, which are summarized in Scheme 1. It is interesting to note that except EMM-23, all the reported extra-large pores zeolites have their largest pores defined by even number of TO_4 tetrahedra. Among the six zeolites with the pore openings larger than 18-rings, four of them (ITQ-54, SYSU-3, ITQ-43 and ITQ-37) contain germanium. Moreover, zeolites with 22- and 26-ring pores are missing.

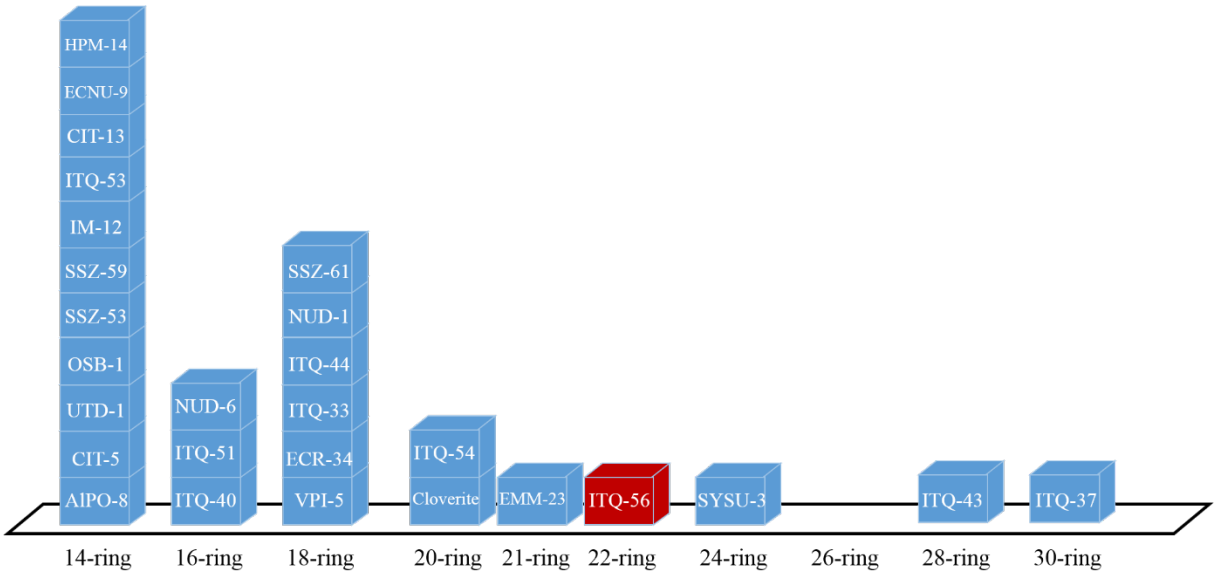

Scheme 1: Pore size distribution of extra-large pore zeolites by ring size opening. ITQ-56 fills the blank of 22-ring.

Although the germanium is a very good candidate to make extra-large pore zeolites,[6] many germanium-rich zeolites are synthesized as polycrystalline powders with crystal sizes too small (< 5 μm) for structure solution by single-crystal X-ray diffraction.[7] Powder X-ray diffraction (PXRD) is also not suitable in this case because of severe peak overlapping and complexity of the structures.[8] Structure determination becomes even more difficult when zeolites have large unit cells, different types of T atoms and contain impurities. Electron crystallography, especially the 3D electron diffraction (ED) techniques, has shown to be a powerful for structure determination of very complex zeolites including germanosilicates.[9,10,11] Recently, a new 3D ED method has been developed where the crystal is continuously rotated with a fast speed while the 3D electron diffraction data are collected. In such an approach, the total data collection time is only a few minutes.[12] The continuous rotation electron diffraction (cRED) allows collection of almost complete high quality 3D ED data from very beam sensitive materials such as germanium-rich zeolites, metal-organic frameworks (MOFs), proteins and small organic

molecules. This provides new opportunities to solve structures that remained unsolved for decades.[13]

N,N,N-trimethyl-adamantammonium TMA-da$^+$ has been demonstrated as an effective OSDA for syntheses of SSZ-13, SSZ-23,[14] and ITQ-1.[15] In the search for new OSDAs for synthesis of extra-large pore zeolites, we discovered that by expansion of the size of OSDAs, it was possible to transform zeolite products from large to extra-large pores.[16] Therefore, we identified memantine with two more methyl groups than adamantamine, which is a drug for anti Alzheimer diseases, as a starting molecule for preparing OSDAs directed to the synthesis of extra-large pore zeolites. Following this idea, we prepared 3,5,N,N,N-pentamethyl-1-adamantammonium and used here as the OSDA. In this work, we report the synthesis of a new germanosilicate zeolite ITQ-56 using 3,5,N,N,N-pentamethyl-1-adamantammonium as the OSDA. The structure was determined from cRED data, which shows that ITQ-56 fills the missing member of extra-large pore zeolite with 22-ring channels.

EXPERIMENTAL METHODS

The 3,5,N,N,N-pentamethyl-1-adamantammonium hydroxide (Figure S1) was synthesized with one step quaternization of memantine. Detailed synthesis of the OSDA can be found in Supporting Information. The novel zeolite ITQ-56 was obtained after crystallization at 200 °C for one day using the 3,5,N,N,N-pentamethyl-1-adamantammonium hydroxide cation as the OSDA, from a synthesis gel with the following composition: $0.667SiO_2$:$0.333GeO_2$:0.15OSDAOH:$0.15NH_4F$:$3H_2O$. Further details about the synthesis of ITQ-56 and the results of final products are given in the Supporting Information and Figure S2. ITQ-56 has plate-like crystals in a size of ~$2.00\times0.50\times0.02$ μm (Figure S9). The plate-like crystals are closely packed in larger building blocks that are surrounded with an amorphous material. Since the sample contained a significant amount of amorphous phase (ca 18%), as

estimated by comparing the CHN analysis and the OSDA contents obtained from the structure refinement.

The sample of ITQ-56 characterized by CHN and ICP analysis, thermogravimetric analysis, PXRD, NMR spectroscopy and Ar and N_2 gas sorption. The details are given in Supporting Information.

Structure analysis by transmission electron microscope (TEM) and continuous rotation electron diffraction (cRED) TEM and cRED investigations were carried out on a JEOL JEM-2100 TEM operated at 200 kV. The powder of ITQ-56 was crushed in an agate mortar, dispersed in an ethanol and treated by sonication for 2 minutes. In order to remove the amorphous phase in the sample, the prepared ITQ-56 suspension was decanted and sonicated several times. A droplet of the suspension was then transferred to a copper EM grid covered by a holey carbon film. A cryo-transfer tomography holder (Gatan 914) was used and the EM sample grid was cooled down to -175^o before insertion into the TEM. The temperature was kept at -175^o during the entire data collection process. The cRED data were collected using SoPhy Software and a highly sensitive hybrid pixel Timepix Quad camera. During the cRED data collection, the goniometer was tilted continuously with a rotation speed of 0.45^o per second and an exposure time for each frame was 0.5 seconds. The cRED datasets were processed using the software XDS developed for X-ray diffraction.[17] The structure of ITQ-56 was solved by direct methods using the software SIR2014,[18] and further refined using software SHELXL-97[19].

Rietveld refinement Synchrotron PXRD data were collected from the *as-made* sample of ITQ-56 at European Synchrotron Radiation Facility (ESRF) in Grenoble (λ= 0.39984 Å). The sample was sealed in a Kapton capillary of 1.00 mm in diameter. Initially, a Pawley fit was performed to optimize unit cell parameters, background and peak shape function. Structure model determined from cRED data was refined against synchrotron PXRD data using TOPAS Academic V5.[20] Data up to 2theta of 18° corresponding to a d-spacing of 1.278 Å were used.

The Rietveld refinement was conducted using Pseudo-Voigt (PV) type peak profile function, and the zero shift, capillary shift, unit cell parameters, atomic positions of T and O atoms, silicon and germanium occupancies and atomic displacement parameters were refined. Geometric restraints were applied for all T-O (1.61 – 1.74 Å) distances and O-T-O (109.5^{o}) angles. Geometric restraints were gradually during the progress of the refinement. Four OSDA molecules were first located manually according to the difference Fourier map. The positions of carbon and nitrogen atoms were later refined using geometric restraints, which were gradually released at the end of the refinement. The fluoride ions were found from the difference Fourier map and their occupancies were refined.

RESULTS AND DISCUSSION

cRED data were collected from many crystals, which show various qualities depending on the crystals. Six cRED datasets with the best statistics were chosen for structure determination of ITQ-56. The six cRED datasets were scaled and merged together into one *hkl* list file and used for structure solution and refinement. The merged dataset has a completeness of 82 % and a resolution up to 1.1 Å, and contains 58235 reflections among which 2903 are unique ($R_{int.}$=0.233) (Table 1). All T and O atoms were found during the structure solution. 246 parameters were refined using 40 geometric restraints for T-O distances and the refinement converged with a final R_1 value of 0.284.

The structure of ITQ-56 has orthorhombic space group *Immm* (71) with very large unit cell parameters *a*=13.5066 Å, *b*=26.5896 Å, *c*=55.5013 Å. It has an exceptionally long *c*-axis that is the fourth longest axis among zeolites published in the Database of Zeolite Structures.[21] Only zeolites IM-5[22] (*b* = 57.2368 Å), AlPO-78[23] (*c*=60.6099 Å) and SSZ-57[24] (*c*=109.7560 Å) have longer axes than ITQ-56. The structure has 19 T atoms that are shared by silicon and germanium (Si/Ge ratio is 1.15 from cRED data) and 49 O atoms per asymmetric unit. The Si/Ge ratio refined from cRED data is lower than the one obtained by ICP, which is due to the presence of

Si-rich amorphous material in the sample. Among 248 zeolite structures in the Database of Zeolite Structures, only ten have more than 19 T atoms in the asymmetric unit. Interestingly, most of these frameworks are disordered (ITQ-39,[25] IPC-6,[26] SSZ-57,[24] SSZ-61,[27] SSZ-31 polymorph I,[28] SSZ-70[29]) and/or are interrupted (ITQ-39,[25] SSZ-61,[27] SSZ-74,[30] SSZ-70[29]).

Table 1. Continuous rotation electron diffraction (cRED) and structure refinement details of ITQ-56.

Crystal system	Orthorhombic
Space group	*Immm* (71)
a, Å	13.51
b, Å	26.40
c, Å	55.09
Volume, Å^3	19648.6
λ, Å	0.0251
Tilt range per frame (°)	0.23
Exposure time per frame (s)	0.5
Completeness, %	82
No. parameters	248
Resolution, Å	1.1
No. restraints	40
R_{int}	0.233
Reflections collected / unique	58235 / 2903
R_1	0.286
wR_2	0.560
GoF	2.38

The structure of zeolite ITQ-56 is built from two different cages. ¨Double¨ [$4^2 5^4 6^2$] cage with one 4-ring in common and two additional dimers at one side, and [$4^6 6^{12}$] cage in which 4-rings at two different orientations with occupancy 0.5 are located (Figure 1a, 1b). The same types of the cages are connected to each other via oxygen atoms to form chains along *a* (Figure 1c, 1d). Two chains containing the same type of cages are paired together along *c*, there is no connection between two "double" [$4^2 5^4 6^2$] cages producing terminal T atoms. The paired chains are then shifted by 0.5 along *a*, *b*, and *c* and connected via oxygen atoms to form the 3D structure (Figure 1e).

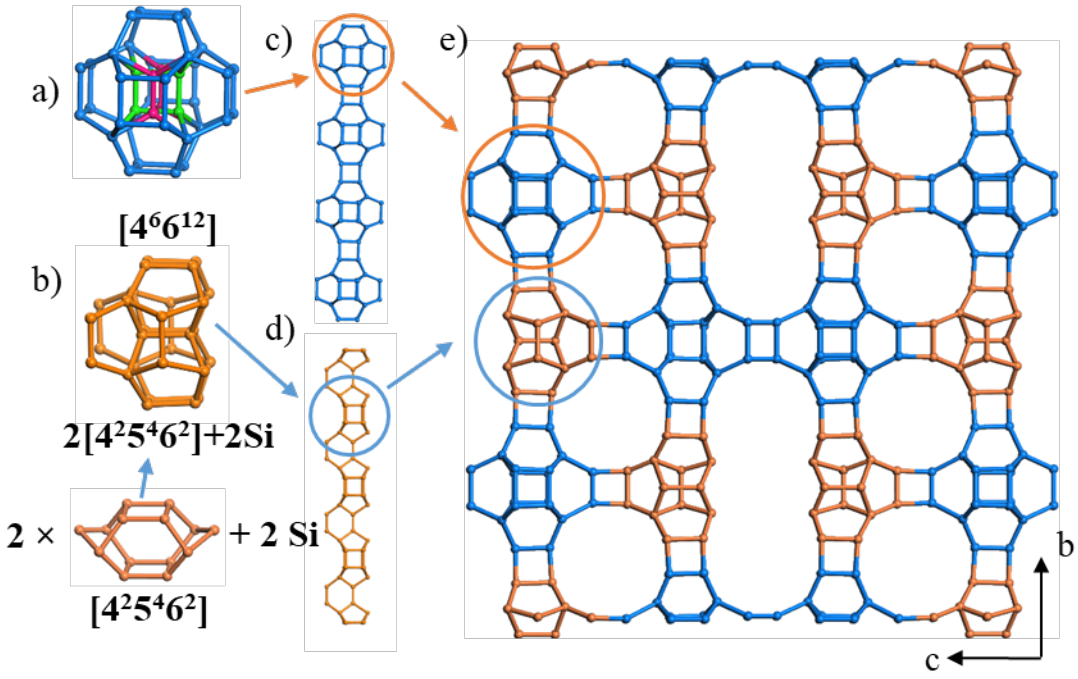

Figure 1. Construction of the ITQ-56 framework. a) Illustrated [$4^6 6^{12}$] cage where different orientations of 4-rings are marked in pink and green colour; b) "double" [$4^2 5^4 6^2$] cage with one 4-ring in common and two additional TO_4 dimers at one side; c) the cage chain of [$4^6 6^{12}$] by connecting them via *d*4*r*s, coloured blue; d) the cage chain of b) by connecting them via two 4-rings, coloured brown; e) 3D framework of zeolite ITQ-56 viewed along [100]. Only the connections of T atoms are shown for clarity.

The structure of ITQ-56 exhibits 3D channel system with extra-large 22-rings along [100]. There are straight 12-ring channels along [100], <110> and <101>. There are also straight 12-ring channel along [010]. The extra-large 22-ring channel are created due to the missing *d*4*r*s. Furthermore, the channels are also interconnected by channel connections. The steric view of channel system is shown in Figure 2a. Pore windows and sizes of channels are presented in Figure S10. The free diameters of 12-ing pore openings are ~7 Å and the extra-large 22-ring has pore sizes of 4.7 Å × 19.9 Å providing a very large cavity in the structure. The structure is also illustrated by tilling and nets as shown in Figure 2b. The ITQ-56 exhibits transitivity of (18)(44)(48)(22), in which 18 independent vertices (omit the disorder in the cage of [$4^6 6^{12}$]), 44

independent edges, 48 independent facet classes, 22 independent tile classes. Among the 22 tile classes, the 12 important classes are also shown in Figure 2b.

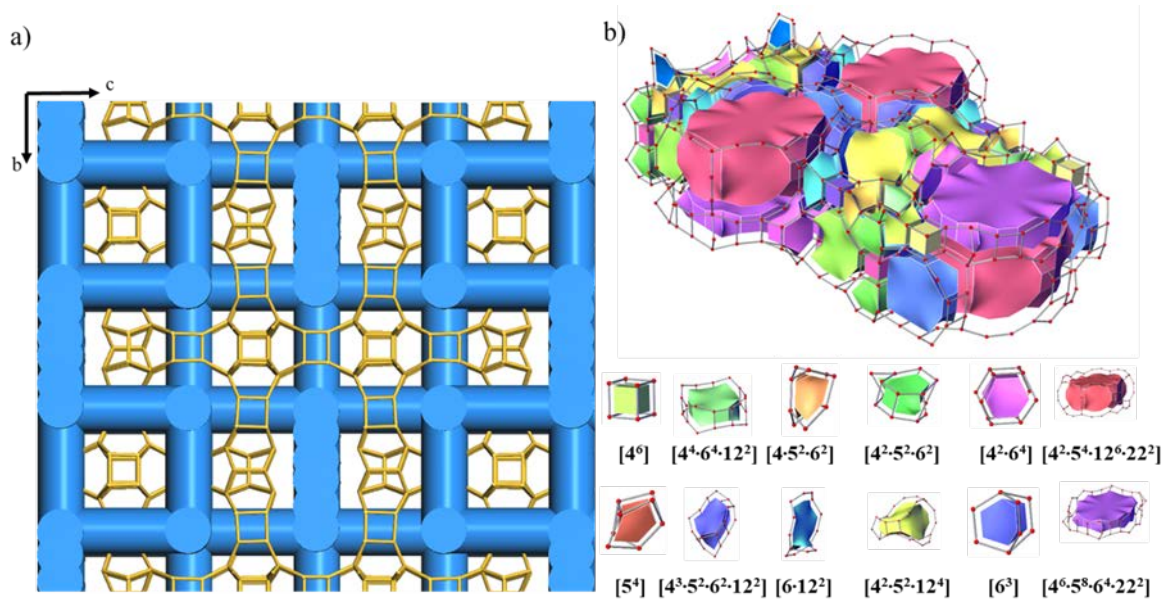

Figure 2. a) The steric view of channel configuration, showing the connections of the 22-ring channels with the 12-ring channels. b) An illustration of the channel system and cavities in the ITQ-56 by tiling and net.

The framework of ITQ-56 is closely related to several zeolites that contain 3D 12-ring channels; ITQ-26 (three letter code IWS[21], space group *I*4/*mmm* (139), *a* = 26.7769 Å and *c* = 13.2505 Å)[31] and ITQ-21 (space group *Fm*-3*c*, a = 27.689 Å)[32] and PKU-14[33]. The projection of ITQ-56 along *c* is very similar to those of ITQ-26 along *a* and *b*. The projection of ITQ-56 along *a* and the projection ITQ-26 along *c* varies with a repetition of the two cages – "double" $[4^2 5^4 6^2]$ cage with one 4-ring in common and $[4^6 6^{12}]$ cage. For ITQ-26 these cages are alternating but for ITQ-56 there is a mirror plane in the middle of *c*-axis producing two similar cages next to each other. There are also some other similar zeolite structures, for example, ITQ-21 that is built entirely of $[4^6 6^{12}]$ cages with *a, b, c* axis oriented disordered interior single 4-ring interconnected via *d*4*r*s. Whereas, the structure of zeolite PKU-14[33] and NUD-3(Chem. Commun. 2021, 2, 191-194) that consists of missing single 4-ring and fully ordered single 4-

ring [$4^6 6^{12}$] cages respectively. The aforementioned zeolites (ITQ-26 and PKU-14) have local disorder in the [$4^6 6^{12}$] cage. In ITQ-26 case, there are 4-rings with three different orientations inside the cage. Zeolite PKU-14 has eight terminal hydroxyl groups located making a large void that can accommodate a $(H_2O)_2$ dimer. In case of ITQ-56, refinement using cRED data shows that there exist two different orientations of 4-ring with an occupancy of 0.5 each, as shown in Figure 1a.

The Pawley fit of synchrotron PXRD data confirmed the space group *Immm* (71) and unit cell parameters. The broad peaks and relatively low resolution of the synchrotron PXRD data (intensities start to decay from 2theta of 10°, d = 2.3 Å) together with the large background from the amorphous impurity in the sample made the Rietveld refinement of such a complex structure very challenging. The Rietveld refinement was done in order to locate OSDA molecules and compare the structure to the one achieved with cRED data.

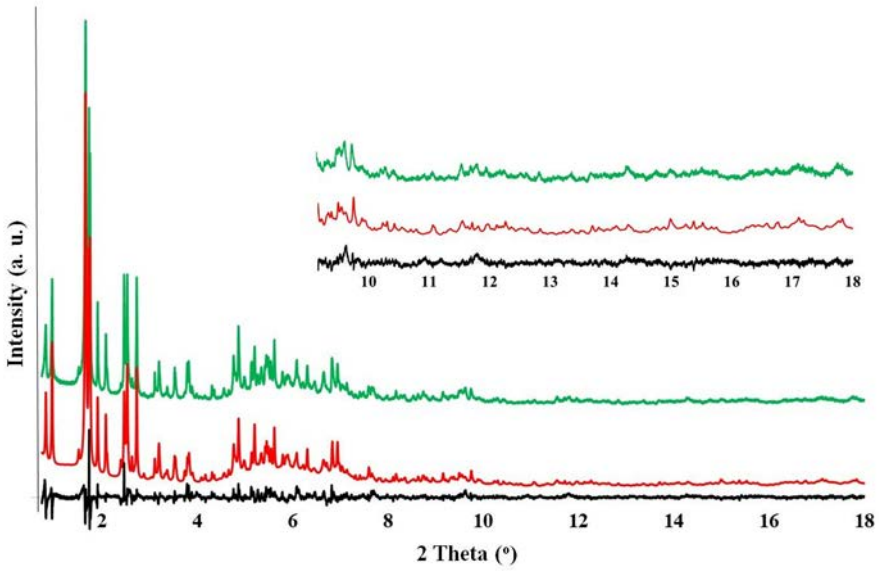

Figure 3. The plots of Rietveld refinement against synchrotron PXRD of the *as-made* ITQ-56, the part from 9 to 18° 2Theta is enlarged by a factor of 3. The curves from top to bottom are observed (green), calculated (red) and difference (black) profiles respectively (λ= 0.39984 Å).

The Rietveld refinement (Figure 3, Table 2) converged to R_{wp}=0.149 and confirmed the structure model of ITQ-56 obtained using the cRED data. The fluoride ions were located in the middle of *d*4*r*s in the difference Fourier map (Figure S11). The OSDA molecules were placed into the pores manually where the residual density is found according to the difference Fourier map (Figure S11). Their positions were refined using geometric restraints, which were gradually released during the refinement. Four symmetry-independent OSDA molecules are located in the pores of ITQ-56 (Figure 4b), two of them are located in the 22-ring channel and two are in the 12-ring channels along [100] and [010], respectively.

The Si/Ge ratio (1.15) after refinement using cRED data (merged from six crystals) is lower than that (1.37) obtained by the Rietveld refinement. The fluoride content from cRED (12.2) and Rietveld refinement (9.6) also differs. This could be due to the sample inhomogeneity. The structure obtained from cRED data were from only six crystals, while the Rietveld refinement was done from the bulk sample. The calculated amount of the OSDA from CHN analysis and Rietveld refinement leads to 18% of the amorphous component in the synthesized material. EDS shows that the amorphous material is Si-rich. This may explain why the Si/Ge ratio in ICP analysis is higher than those obtained by the structure refinement of ITQ-56.

Table 2. The details of Rietveld refinement of as-made ITQ-56.

Crystal system	Orthorhombic
Space group	*Immm* (71)
a, Å	13.5076
b, Å	26.5882
c, Å	55.4883
λ, Å	0.39984
Temperature, ^{o}C	20
2Theta range, ^{o}	0.75-20.0
Resolution, Å	1.15
No. of restraints	78 for T-O, 120 for O-T-O, 46 T-O-T
No. of reflections	3807
R_{wp}	0.149
R_{exp}	0.566
GoF	2.64

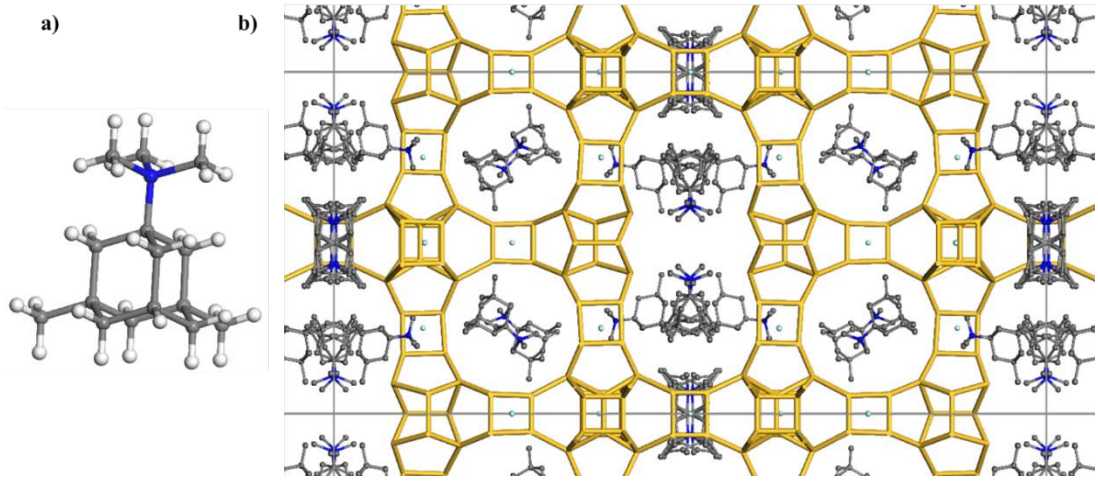

Figure 4. a) The OSDA molecule used for synthesis of ITQ-56, carbon atoms are presented in grey, a nitrogen atom in blue and hydrogen atoms in white and b) location of OSDA molecules in the structure of ITQ-56.

The extra-large channels with 22-ring opening in ITQ-56 are formed due to a missing *d*4*r* unit in the center of the 22-ring (Figure 5a). If the missing *d*4*r* unit is added, a fully 4-connected 3D framework with 3D intersecting 12-ring channels is formed (Figure 5b). Most probably, the missing d4r unit is due to the OSDA molecule used in the synthesis of ITQ-56, which is both large and bulky (Figure 4a). The large OSDA could be an important factor for the formation of the 22-ring. In the synthesis of ITQ-21, ITQ-26 and PKU-14 with 3D 12-ring channels, the sizes of the OSDA molecules (N(16)-methylsparteinium hydroxide for ITQ-21, 1,3-bis-(triethylphosphoniummethyl)-benzene for ITQ-26 and dicyclohexyldimethylammonium hydroxide for PKU-14) are smaller and can fit in the 12-ring channels. With a proper selection of OSDAs, the fully connected ITQ-56_FULL structure may be synthesized. The discovery of ITQ-56 demonstrated a new approach of making extra-large pore zeolites, i.e. by introducing ordered defects in zeolite frameworks. In the case of ITQ-56, by selective removal of d4r units

in the framework. It is worth mentioning that cRED data show no evidence of defects, indicating that the removal of *d*4*r*s is highly ordered.

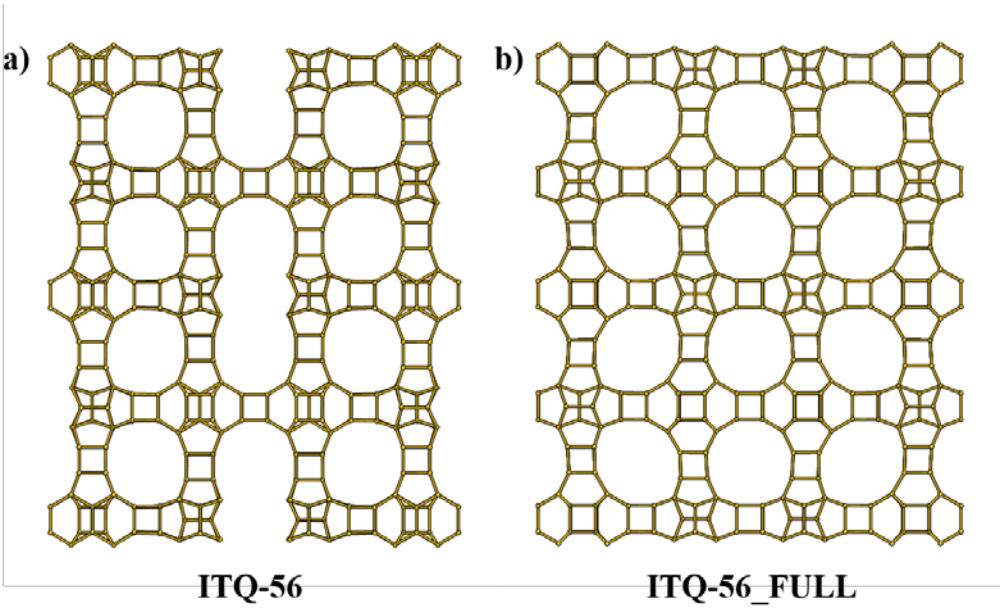

Figure 5. Comparison of the ITQ-56 framework (a) with a hypothetic fully-connected zeolite framework deduced from ITQ-56 (b). Only T-T connections are shown for clarity.

The chemical analysis of the sample indicates that the OSDA is intact in the pores, with a C/N ratio of 14.9, which is close to the theoretical value of 15. This is further confirmed by the good agreement between ^{13}C liquid NMR of the OSDA and ^{13}C-MAS-NMR of ITQ-56 (Figure S3). ICP analysis of the solids obtained gives a Si/Ge ratio of 2.24. When carrying out the ^{29}Si MAS NMR analysis, the selective enhancement of the signal at 100.8 ppm with a shoulder at about -93ppm in Si cross polarization (CP) MAS-NMR comparing to ^{29}Si Bloch decay (BD) MAS-NMR spectra (Figure S4) of the *as-made* sample implies the presence of Q3 (≡Si – OH) species. The ^{19}F MAS-NMR spectrum (Figure S5) shows a single resonance band at -8.42 ppm, indicating that fluorine anions are trapped in the *d*4*r*s. Pore size argon adsorption gives a peak centered at 0.71 nm with a shoulder at 0.85 nm that may correspond to the cyclic 12-ring large pore and elliptical 22-ring extra-large pore, respectively. Nitrogen adsorption measurements

gave a BET surface area of 484.2 m^2/g. The actual BET surface of ITQ-56 is higher, owing to the presence of the amorphous solid in the sample and some loss of crystallinity during the calcination process (Figure S6). The thermogravimetric analysis of the *as-made* ITQ-56 shows a total weight loss of 17.2 wt%, which corresponds to the organic OSDA and F^- ions occluded within the zeolite (Figure S7). The crystallinity of ITQ-56 was retained after calcination up to 600 ^oC under dry air atmosphere (Figure S8).

CONCLUSIONS

The first zeolite containing extra-large 22-ring channels has been synthesized using a modified memantine as the organic structure directing agent (OSDA). The structure of ITQ-56 is complex and has exceptionally large unit cell parameter. The framework structure of ITQ-56 was determined by continuous rotation electron diffraction (cRED), and the OSDAs were located by Rietveld refinement using synchrotron powder X-ray diffraction data. The framework of ITQ-56 contains a 3D 22×12×12 channel system, and is closely related to several zeolites that contain 3D 12-ring channels. We show that highly ordered extra-large pore zeolites can be synthesized by systematic removal of *d*4*r* units in zeolite frameworks – a new approach of making novel zeolite frameworks. The discovery of ITQ-56 fills the space of "missing 22-ring chain" among the extra-large pore zeolites.

ACKNOWLEDGMENTS

This work has been supported by the European Union through ERC-AdG-2014-671093 (SynCatMatch), by the Spanish Government-MINECO through ''Severo Ochoa" (SEV-2016-0683), the Swedish Research Council (VR, 2017-04321) and the Knut & Alice Wallenberg Foundation through the project grant 3DEM-NATUR (KAW, 2012-0112). The EM facility was supported by the Knut and Alice Wallenberg Foundation. TW acknowledges the Swedish

Research Council (VR) for an International Postdoc grant (2014-06948). JJ thanks the Youth 1000 Talents Program of China; the National Natural Science Foundation 21971259. We thank Lynne McCusker for help and initial guidance of the Rietveld refinement.

References

1. Burton, A. W., Zones, S. I. & Elomari, S. The chemistry of phase selectivity in the synthesis of high-silica zeolites. *Curr. Opin. Colloid Interface Sci.* **10**, 211–219 (2005).
2. Gallego, E. M. *et al.* "Ab initio" synthesis of zeolites for preestablished catalytic reactions. *Science* **355**, 1051–1054 (2017).
3. Jiang, J., Yu, J. & Corma, A. Extra-Large-Pore Zeolites: Bridging the Gap between Micro and Mesoporous Structures. *Angew. Chem. Int. Ed.* **49**, 3120–3145 (2010).
4. Eliášová, P. *et al.* The ADOR mechanism for the synthesis of new zeolites. *Chem. Soc. Rev.* **44**, 7177–7206 (2015).
5. Yang, B. *et al.* Synthesis of Extra-Large-Pore Zeolite ECNU-9 with Intersecting 14*12-Ring Channels. *Angew. Chem. Int. Ed.* **57**, 9515–9519 (2018).
6. Bai, R. *et al.* Simple Quaternary Ammonium Cations-Templated Syntheses of Extra-Large Pore Germanosilicate Zeolites. *Chem. Mater.* **28**, 6455–6458 (2016).
7. Sun, J. *et al.* The ITQ-37 mesoporous chiral zeolite. *Nature* **458**, 1154–1157 (2009).
8. Willhammar, T., Yun, Y. & Zou, X. Structural Determination of Ordered Porous Solids by Electron Crystallography. *Adv. Funct. Mater.* **24**, 182–199 (2014).
9. Hua, W. *et al.* A Germanosilicate Structure with 11×11×12-Ring Channels Solved by Electron Crystallography. *Angew. Chem. Int. Ed.* **53**, 5868–5871 (2014).
10. Su, J. *et al.* Structure analysis of zeolites by rotation electron diffraction (RED). *Microporous Mesoporous Mater.* **189**, 115–125 (2014).
11. Jiang, J., Yun, Y., Zou, X., Luis Jorda, J. & Corma, A. ITQ-54: a multi-dimensional extra-large pore zeolite with 20 × 14 × 12-ring channels. *Chem. Sci.* **6**, 480–485 (2015).
12. Simancas, J. *et al.* Ultrafast Electron Diffraction Tomography for Structure Determination of the New Zeolite ITQ-58. *J. Am. Chem. Soc.* **138**, 10116–10119 (2016).
13. Wang, Y. *et al.* Elucidation of the elusive structure and formula of the active pharmaceutical ingredient bismuth subgallate by continuous rotation electron diffraction. *Chem. Commun.* **53**, 7018–7021 (2017).
14. Camblor, M. A. *et al.* SSZ-23: An Odd Zeolite with Pore Openings of Seven and Nine Tetrahedral Atoms. *Angew. Chem. Int. Ed.* **37**, 2122–2126 (1998).

15. Camblor, M. A., Corma, A., Díaz-Cabañas, M.-J. & Baerlocher, C. Synthesis and Structural Characterization of MWW Type Zeolite ITQ-1, the Pure Silica Analog of MCM-22 and SSZ-25. *J. Phys. Chem. B* **102**, 44–51 (1998).

16. Jiang, J. *et al.* Investigation of Extra-Large Pore Zeolite Synthesis by a High-Throughput Approach. *Chem. Mater.* **23**, 4709–4715 (2011).

17. Kabsch, W. XDS. *Acta Crystallogr. D Biol. Crystallogr.* **66**, 125–132 (2010).

18. Burla, M. C. *et al. SIR2011* : a new package for crystal structure determination and refinement. *J. Appl. Crystallogr.* **45**, 357–361 (2012).

19. Sheldrick, G. M. Crystal structure refinement with SHELXL. *Acta Crystallogr. Sect. C Struct. Chem.* **71**, 3–8 (2015).

20. Coelho, A. A. *TOPAS* and *TOPAS-Academic* : an optimization program integrating computer algebra and crystallographic objects written in C++. *J. Appl. Crystallogr.* **51**, 210–218 (2018).

21. Database of Zeolite Structures. http://www.iza-structure.org/databases/.

22. Baerlocher, C. *et al.* Structure of the Polycrystalline Zeolite Catalyst IM-5 Solved by Enhanced Charge Flipping. *Science* **315**, 1113–1116 (2007).

23. Yuhas, B. D., Mowat, J. P. S., Miller, M. A. & Sinkler, W. AlPO-78: A 24-Layer ABC-6 Aluminophosphate Synthesized Using a Simple Structure-Directing Agent. *Chem. Mater.* **30**, 582–586 (2018).

24. Baerlocher, C., Weber, T., McCusker, L. B., Palatinus, L. & Zones, S. I. Unraveling the Perplexing Structure of the Zeolite SSZ-57. *Science* **333**, 1134–1137 (2011).

25. Willhammar, T. *et al.* Structure and catalytic properties of the most complex intergrown zeolite ITQ-39 determined by electron crystallography. *Nat. Chem.* **4**, 188–194 (2012).

26. Morris, S. A. *et al.* In situ solid-state NMR and XRD studies of the ADOR process and the unusual structure of zeolite IPC-6. *Nat. Chem.* **9**, 1012–1018 (2017).

27. Smeets, S. *et al.* High-Silica Zeolite SSZ-61 with Dumbbell-Shaped Extra-Large-Pore Channels. *Angew. Chem. Int. Ed.* **53**, 10398–10402 (2014).

28. Lobo, R. F. *et al.* A Model for the Structure of the Large-Pore Zeolite SSZ-31. *J. Am. Chem. Soc.* **119**, 3732–3744 (1997).

29. Smeets, S. *et al.* Well-Defined Silanols in the Structure of the Calcined High-Silica Zeolite SSZ-70: New Understanding of a Successful Catalytic Material. *J. Am. Chem. Soc.* **139**, 16803–16812 (2017).

30. Baerlocher, C. *et al.* Ordered silicon vacancies in the framework structure of the zeolite catalyst SSZ-74. *Nat. Mater.* **7**, 631–635 (2008).

31. Dorset, D. L. *et al.* Crystal Structure of ITQ-26, a 3D Framework with Extra-Large Pores. *Chem. Mater.* **20**, 5325–5331 (2008).

32. Corma, A., Díaz-Cabañas, M. J., Martínez-Triguero, J., Rey, F. & Rius, J. A large-cavity zeolite with wide pore windows and potential as an oil refining catalyst. *Nature* **418**, 514–517 (2002).

33. Liang, J. *et al.* A 3D 12-Ring Zeolite with Ordered 4-Ring Vacancies Occupied by (H2O)2 Dimers. *Chem. – Eur. J.* **20**, 16097–16101 (2014).

An extra-large pore zeolite ITQ-56 has been synthesized and its structure has been elucidated by continuous rotation electron diffraction data

Elina Kapaca[†,#], Jiuxing Jiang[§,#], Jose L. Jorda[⊥], Maria J. Diaz-Cabañas[⊥], Xiaodong Zou[†], Avelino Corma[⊥,*], Tom Willhammar[†,*]

Page No. – Page No.